Available online at www.sciencedirect.com
ScienceDirect
Computers and Mathematics with Applications 55 (2008) 1568–1575
An International Journal
computers & mathematics
with applications
www.elsevier.com/locate/camwa

A new scheme for source term in LBGK model for convection–diffusion equation

Baochang Shi[a,b,*], Bin Deng[a], Rui Du[b], Xingwang Chen[a]

[a] *Department of Mathematics, Huazhong University of Science and Technology, Wuhan 430074, PR China*
[b] *State Key Laboratory of Coal Combustion, Huazhong University of Science and Technology, Wuhan 430074, PR China*

Abstract

A new scheme for source term in the lattice BGK (LBGK) model for convection–diffusion equation is proposed. Unlike the models proposed previously, the present scheme only requires the source term in order of the Knudsen number by adding a differential operator of the source term to the evolution equation. The scheme can be applied to reaction–diffusion systems directly. Numerical results are found to be in excellent agreement with the analytical solutions. It is also found that the numerical accuracy of the present scheme is generally much better than that of the existing models.

Keywords: Lattice BGK model; Convection–diffusion equation with source; Reaction–diffusion system

1. Introduction

The lattice Boltzmann method (LBM) is a new technique for simulating fluid flows and modeling complex physics in fluids [1]. Compared with the conventional computational fluid dynamics approach, the LBM is easy for programming, intrinsically parallel, and it is also easy to incorporate complicated boundary conditions such as those in porous media. In the past years, the lattice BGK (LBGK) model, the most popular LBM, has achieved great success in a variety of fields, ranging from simple laminar flows to thermal flows [2,3], compressible flows [4], porous media [5,6], blood flow and particle suspensions [7,8], and so on. The LBM also shows potentials to simulate the non-linear systems, including reaction–diffusion equation (RDE) [9,10], convection–diffusion equation (CDE) [11–13] and wave equation [14]. However, they are limited to isotropic diffusion. Recently, the LB models for advection and anisotropic dispersion equation have been proposed [15–17], among them the model by Ginzburg [17] is generic, which extends the generalized or multi-relaxation-times LB model [18,19] to the advection and anisotropic dispersion equation.

In the treatment of source term in the existing LB models for CDE/RDE, the assumption that $F(\mathbf{x}, t) \propto \epsilon^2$ was needed [9,10,17], where ϵ is the Knudsen number. If the assumption is weaken as $F(\mathbf{x}, t) \propto \epsilon$ which was used in the common LB models for Navier–Stokes equation with source or force term, the additional term may appear in the derived macroscopic equation as showed in Ref. [20].

* Corresponding author at: Department of Mathematics, Huazhong University of Science and Technology, Wuhan 430074, PR China.
E-mail address: sbchust@yahoo.com (B. Shi).

0898-1221/$ - see front matter © 2007 Elsevier Ltd. All rights reserved.
doi:10.1016/j.camwa.2007.08.016

In this paper, we present a new scheme for source term in the LBGK model for CDE by adding a differential operator of the source term to the evolution equation. The scheme only requires $F(\mathbf{x}, t) \propto \epsilon$, and can be applied to reaction–diffusion systems directly. Numerical results are found to be in excellent agreement with the analytical solutions. It is also found that the numerical accuracy of the present scheme is generally much better than that of the existing models.

2. LBGK model

The n-dimensional (nD) CDE with source term considered in this paper can be written as

$$\partial_t \rho + \mathbf{u} \cdot \nabla \rho = \alpha \nabla^2 \rho + F(\mathbf{x}, t), \tag{1}$$

where $\mathbf{u} = (u_1, u_2, \ldots, u_n)^T$ is a constant vector of length n, α is the diffusion coefficient, ∇ is the gradient operator with respect to the spatial coordinate $\mathbf{x}$ in dimensions and ∇^2 is the corresponding Laplacian operator. ρ is the density at time t and position $\mathbf{x}$. $F(\mathbf{x}, t)$ is the source term. When $\mathbf{u} = 0$, Eq. (1) becomes the diffusion equation (DE) with source term, and several of such equations form a reaction–diffusion system (RDS).

Our LBGK scheme is based on the DnQb lattice [1] in the LBGK model with b velocity directions in nD space and treats the source term in a different way.

The evolution equation of the distribution function in the model reads

$$f_i(\mathbf{x} + \mathbf{c}_i \Delta t, t + \Delta t) - f_i(\mathbf{x}, t) = -\frac{1}{\tau}(f_i(\mathbf{x}, t) - f_i^{\mathrm{eq}}(\mathbf{x}, t)) + \Delta t F_i(\mathbf{x}, t) + \frac{\Delta t^2}{2}\overline{D}_i F_i(\mathbf{x}, t),$$
$$i = 0, \ldots, b-1, \tag{2}$$

where $\overline{D}_i = \partial_t + \theta \mathbf{c}_i \cdot \nabla$, $\theta \in [0, 1]$ is a parameter corresponding to different schemes. $\{\mathbf{c}_i, i = 0, \ldots, b-1\}$ is the set of discrete velocity directions, Δx and Δt are the lattice spacing and the time step, respectively, $c = \Delta x / \Delta t$ is the particle speed, τ is the dimensionless relaxation time, and $f_i^{\mathrm{eq}}(\mathbf{x}, t)$ is the equilibrium distribution function which is determined by

$$f_i^{\mathrm{eq}}(\mathbf{x}, t) = \omega_i \rho \left(1 + \frac{\mathbf{c}_i \cdot \mathbf{u}}{c_s^2} + \frac{(\mathbf{c}_i \cdot \mathbf{u})^2}{2c_s^4} - \frac{|\mathbf{u}|^2}{2c_s^2}\right), \tag{3}$$

where ω_i are weights and c_s, the so-called sound speed in LBM for fluids, is related to c and ω_i. They depend on the lattice model used.

For the D2Q9 model, $\omega_0 = 4/9$, $\omega_{1\sim4} = 1/9$, $\omega_{5\sim8} = 1/36$, for the D3Q15 one, $\omega_0 = 2/9$, $\omega_{1\sim6} = 1/9$, $\omega_{7\sim14} = 1/72$, then $c_s^2 = c^2/3$ for both of them.

$f_i(\mathbf{x}, t)$ and $f_i^{\mathrm{eq}}(\mathbf{x}, t)$ satisfy

$$\sum_i f_i = \sum_i f_i^{\mathrm{eq}} = \rho, \qquad \sum_i \mathbf{c}_i f_i^{\mathrm{eq}} = \rho \mathbf{u}, \qquad \sum_i \mathbf{c}_i \mathbf{c}_i f_i^{\mathrm{eq}} = \rho \mathbf{u}\mathbf{u} + c_s^2 \rho \mathbf{I}, \tag{4}$$

where $\mathbf{I}$ is the unit tensor.

The corresponding source term F_i is taken as

$$F_i = \omega_i F \left(1 + \frac{\tau - \frac{1}{2}}{\tau - \frac{\theta}{2}} \frac{\mathbf{c}_i \cdot \mathbf{u}}{c_s^2}\right) \tag{5}$$

such that $\sum_i F_i = F$, $\sum_i \mathbf{c}_i F_i = \frac{\tau - \frac{1}{2}}{\tau - \frac{\theta}{2}} F \mathbf{u}$.

Unlike the existing models, we add $\frac{\Delta t^2}{2}\overline{D}_i F_i(\mathbf{x}, t)$ to the right hand of the evolution equation.

To derive the macroscopic equation (1), the Chapman–Enskog expansion in time and space is applied:

$$f_i = f_i^{\mathrm{eq}} + \epsilon f_i^{(1)} + \epsilon^2 f_i^{(2)}, \qquad F = \epsilon F^{(1)}, \qquad \partial_t = \epsilon \partial_{t_1} + \epsilon^2 \partial_{t_2}, \qquad \nabla = \epsilon \nabla_1, \tag{6}$$

where ϵ is the Knudsen number, a small number. Note that here F is assumed that $F \propto \epsilon$.

Using Eq. (6) and the first formula in Eqs. (4) and (5), we have

$$\sum_i f_i^{(k)} = 0 \quad (k \geq 1), \qquad \sum_i F_i^{(1)} = F^{(1)}, \qquad \sum_i \mathbf{c}_i F_i^{(1)} = \frac{\tau - \frac{1}{2}}{\tau - \frac{\theta}{2}} F^{(1)}\mathbf{u}, \tag{7}$$

where $F_i^{(1)} = \omega_i F^{(1)}(1 + \frac{\tau-\frac{1}{2}}{\tau-\frac{\theta}{2}} \frac{\mathbf{c}_i \cdot \mathbf{u}}{c_s^2})$.

Applying Taylor expansion to Eq. (2), we have

$$D_i f_i + \frac{\Delta t}{2} D_i^2 f_i + \cdots = -\frac{1}{\tau \Delta t}(f_i - f_i^{\mathrm{eq}}) + F_i + \frac{\Delta t}{2} \overline{D}_i F_i, \tag{8}$$

where $D_i = \partial_t + \mathbf{c}_i \cdot \nabla$.

Denote $D_{1i} = \partial_{t_1} + \mathbf{c}_i \cdot \nabla_1$, $\overline{D}_{1i} = \partial_{t_1} + \theta \mathbf{c}_i \cdot \nabla_1$. Substituting Eq. (6) into Eq. (8) and treating the terms in order of ϵ and ϵ^2 separately gives

$$D_{1i} f_i^{\mathrm{eq}} = -\frac{1}{\tau \Delta t} f_i^{(1)} + F_i^{(1)}, \tag{9a}$$

$$\partial_{t_2} f_i^{\mathrm{eq}} + D_{1i} f_i^{(1)} + \frac{\Delta t}{2} D_{1i}^2 f_i^{\mathrm{eq}} = -\frac{1}{\tau \Delta t} f_i^{(2)} + \frac{\Delta t}{2} \overline{D}_{1i} F_i^{(1)}. \tag{9b}$$

Applying Eq. (9a) to the left side of Eq. (9b), we can rewrite Eq. (9b) as

$$\partial_{t_2} f_i^{\mathrm{eq}} + \left(1 - \frac{1}{2\tau}\right) D_{1i} f_i^{(1)} + \frac{\Delta t}{2} D_{1i} F_i^{(1)} = -\frac{1}{\tau \Delta t} f_i^{(2)} + \frac{\Delta t}{2} \overline{D}_{1i} F_i^{(1)}. \tag{10}$$

Then, we have

$$\partial_{t_2} f_i^{\mathrm{eq}} + \left(1 - \frac{1}{2\tau}\right) D_{1i} f_i^{(1)} = -\frac{1}{\tau \Delta t} f_i^{(2)} + \frac{\Delta t}{2}(\theta - 1)\mathbf{c}_i \cdot \nabla_1 F_i^{(1)}. \tag{11}$$

Summing Eqs. (9a) and (11) over i and using Eqs. (4) and (7), we have

$$\partial_{t_1} \rho + \nabla_1 \cdot (\rho \mathbf{u}) = F^{(1)}, \tag{12}$$

$$\partial_{t_2} \rho + \left(1 - \frac{1}{2\tau}\right) \nabla_1 \cdot \sum_i \mathbf{c}_i f_i^{(1)} = \frac{\Delta t}{2}(\theta - 1) \frac{\tau - \frac{1}{2}}{\tau - \frac{\theta}{2}} \nabla_1 \cdot (F^{(1)}\mathbf{u}). \tag{13}$$

Using Eqs. (9a), (4) and (7), we have

$$\begin{aligned} \sum_i \mathbf{c}_i f_i^{(1)} &= -\tau \Delta t \sum_i \mathbf{c}_i (D_{1i} f_i^{\mathrm{eq}} - F_i^{(1)}) \\ &= -\tau \Delta t \left(\partial_{t_1}(\rho \mathbf{u}) + \nabla_1 \cdot (c_s^2 \rho \mathbf{I} + \rho \mathbf{u}\mathbf{u}) - \frac{\tau - \frac{1}{2}}{\tau - \frac{\theta}{2}} F^{(1)}\mathbf{u} \right). \end{aligned} \tag{14}$$

Since $\mathbf{u}$ is a constant vector, it follows from Eq. (12) that

$$\begin{aligned} \sum_i \mathbf{c}_i f_i^{(1)} &= -\tau \Delta t \left(\mathbf{u}(\partial_{t_1} \rho + \nabla_1 \cdot (\rho \mathbf{u})) - \frac{\tau - \frac{1}{2}}{\tau - \frac{\theta}{2}} F^{(1)}\mathbf{u} + c_s^2 \nabla_1 \rho \right) \\ &= -\tau \Delta t \left(c_s^2 \nabla_1 \rho + \frac{1 - \theta}{2(\tau - \frac{\theta}{2})} F^{(1)}\mathbf{u} \right). \end{aligned} \tag{15}$$

So substituting Eq. (15) into Eq. (13) we obtain

$$\partial_{t_2} \rho = \Delta t \left(\tau - \frac{1}{2}\right) c_s^2 \nabla_1^2 \rho. \tag{16}$$

Therefore, combining Eq. (16) with Eq. (12), we have

$$\partial_t \rho + \nabla \cdot (\rho \mathbf{u}) = \alpha \nabla^2 \rho + F, \tag{17}$$

where $\alpha = \Delta t(\tau - \frac{1}{2})c_s^2$ is the diffusion coefficient.

Remark 1. From the above analysis, we can see that there is no additional term found in Eq. (17). If the term $(1/2)\Delta t^2 \overline{D}_i F_i(\mathbf{x}, t)$ is not included in Eq. (2), there must have an additional term $(\Delta t/2)\varepsilon \partial_{t_1} F$ in Eq. (17). However, if F is assumed that $F \propto \epsilon^2$, the source term appears in Eqs. (9b) and (10), not in Eq. (9a). At this time there is no $D_{1i} F_i^{(1)}$ term in Eq. (10), thus the term $(1/2)\Delta t^2 \overline{D}_i F_i(\mathbf{x}, t)$ is not needed in Eqs. (2) and (17) can also be derived.

Remark 2. When $\mathbf{u} = 0$, F_i defined by Eq. (5) is independent of θ. For this case, the DnQ($2n$) or DnQ($2n+1$) lattice model can be used, which leads to the simpler LBKG model.

3. Simulation results

To test the LBGK scheme proposed in the above section, numerical simulations of DE and CDE with source term are carried out. In simulations, the analytic differential value and two difference schemes are used for computing $\overline{D}_i F_i(\mathbf{x}, t)$:

Forward scheme

$$\begin{aligned} &\partial_t F_i(\mathbf{x}, t) = (F_i(\mathbf{x}, t) - F_i(\mathbf{x}, t - \Delta t))/\Delta t, \qquad \theta = 0, \\ &D_i F_i(\mathbf{x}, t) = (F_i(\mathbf{x}, t) - F_i(\mathbf{x} - \mathbf{c}_i \Delta t, t - \Delta t))/\Delta t, \qquad \theta = 1. \end{aligned} \tag{18}$$

Backward scheme

$$\begin{aligned} &\partial_t F_i(\mathbf{x}, t) = (F_i(\mathbf{x}, t + \Delta t) - F_i(\mathbf{x}, t))/\Delta t, \qquad \theta = 0, \\ &D_i F_i(\mathbf{x}, t) = (F_i(\mathbf{x} + \mathbf{c}_i \Delta t, t + \Delta t) - F_i(\mathbf{x}, t))/\Delta t, \qquad \theta = 1. \end{aligned} \tag{19}$$

Other difference schemes can also be used. Note that if $F_i(\mathbf{x}, t + \Delta t)$ is not known at t, the backward scheme is implicit. Since $\overline{D}_i F_i(\mathbf{x}, t)$ is a convex combination of $\partial_t F_i(\mathbf{x}, t)$ and $D_i F_i(\mathbf{x}, t)$, we only consider these two cases, that is, $\theta = 0$ and $\theta = 1$.

The boundary conditions of the non-equilibrium extrapolation scheme by Guo et al. [21] are used.

First, we consider the following 2D DE in a dimensionless form

$$\partial_t \rho = \frac{1}{R_s} \nabla^2 \rho + \rho, \tag{20}$$

where $R_s = L^2/(\alpha T_s)$, L is characteristic length and T_s is characteristic time for the source to provide ρ. In a 2×2 periodic box the solution are given by

$$\rho_{mn} = \exp\left(\left(1 - \frac{(m^2 + n^2)\pi^2}{R_s}\right) t\right) \exp(j\pi(mx + ny)), \tag{21}$$

where $j^2 = -1$ and m and n are integers.

Since ρ_{mn} have similar properties for different m and n, we take the imaginary part of ρ_{mn} and set $m = n = 1$, which gives the following analytical solution:

$$\rho(x, y; t) = \exp\left(\left(1 - \frac{2\pi^2}{R_s}\right) t\right) \sin(\pi(x + y)), \qquad \mathbf{x} = (x, y) \in [0, 2] \times [0, 2]. \tag{22}$$

The initial and boundary conditions are determined by the analytical solution.

Table 1
Comparison of global relative errors (a: $\theta = 0$; b: $\theta = 1$)

R_s		Our model				Model 1	
		Forward 1	Forward 2	Backward	Analytic	Case 1	Case 2
$R_s = 10$	a	0.0143	0.0248	0.0143	0.0143	0.0145	0.0252
	b	0.0147	0.0255	0.0147	0.0148		
$R_s = 100$	a	5.2578e−5	8.4764e−5	5.2393e−5	5.2484e−5	2.7196e−4	4.2332e−4
	b	1.8101e−6	1.3501e−6	1.9354e−6	5.5585e−5		
$R_s = 1000$	a	1.0318e−4	2.0183e−4	1.0290e−4	1.0303e−4	3.9854e−4	6.6254e−4
	b	9.7091e−5	1.9250e−4	9.6802e−5	3.6929e−5		
$R_s = 10\,000$	a	9.0947e−5	1.8800e−4	9.0639e−5	9.0947e−5	4.0026e−4	6.7174e−4
	b	9.0193e−5	1.8694e−4	8.9931e−5	2.8229e−5		

Two cases for computing $\partial_t F_i$ or $D_i F_i$ are considered:

Case 1. $F(x, y; t) = \exp((1 - \frac{2\pi^2}{R_s})t)\sin(\pi(x + y))$ is known;

Case 2. $F(x, y; t) = \rho(x, y; t)$ is unknown. This case is commonly met in RDE/RDS.

In simulations, the analytic differential value, the forward scheme and the backward scheme are used to compute $\partial_t F_i$ or $D_i F_i$, respectively, in Eq. (2) for Case 1 and the forward scheme are used for Case 2. We choose 256×256 grids, $\Delta t = 0.001$, a medium resolution.

Table 1 shows a comparison of global relative error between our scheme and the model without differential operator in Eq. (2), which is denoted by Model 1, with different parameters at 1000 time steps. The global relative error is defined as:

$$E = \frac{\sum_j |\rho(\mathbf{x}_j, t) - \rho^*(\mathbf{x}_j, t)|}{\sum_j \rho^*(\mathbf{x}_j, t)}, \tag{23}$$

where ρ and ρ^* are the numerical solution and analytical one, respectively, and the summation is taken over all grid points. In the table, Forward 1 and Forward 2 are corresponding to the forward schemes used for Case 1 and Case 2, respectively.

It is shown in Table 1 that for the case $(1 - 2\pi^2/R_s) < 0$ (for $R_s = 10$) the errors of our scheme and Model 1 are almost same. This is because that F tends to zero as t increases, and for large R_s such that $(1 - 2\pi^2/R_s) > 0$, F tends to infinite as t increases, our scheme is more accurate. Moreover, the computing errors for Case 2 are larger than those for Case 1 due to the numerical solutions used for the source term. We also simulate Eq. (20) with Eq. (22) in higher resolution and find that the analysis results above are still valid.

The second test problem is the following CDE which is related to Eq. (20) in contrast:

$$\partial_t \rho + \mathbf{u} \cdot \nabla \rho = \frac{1}{Pe}\nabla^2 \rho + F(\mathbf{x}, t), \quad \mathbf{x} = (x, y) \in [0, 2] \times [0, 2]. \tag{24}$$

Analytical solution of Eq. (24) is also taken the form as Eq. (22)

$$\rho(x, y; t) = \exp((1 - 2\pi^2/Pe)t)\sin(\pi(x + y)), \tag{25}$$

which leads to the following source term

$$F(x, y; t) = \exp((1 - 2\pi^2/Pe)t)(\pi(u_1 + u_2)\cos(\pi(x + y)) + \sin(\pi(x + y))), \tag{26}$$

where $\mathbf{u} = (u_1, u_2)^T$ and $Pe = LU/\alpha$ is the Peclet number. L and U are characteristic length and velocity, respectively. The boundary and initial conditions are the same as the problem (20).

Since F is known, the forward scheme, backward scheme, and analytic differential value are used for computing $\partial_t F_i$ or $D_i F_i$ in Eq. (2).

Table 2
Comparison of global relative errors (a: $\theta = 0$; b: $\theta = 1$)

Parameters		Our model			Model 1
		Forward	Backward	Analytic	
$u = 0.01, Pe = 10$	a	0.0143	0.0143	0.0143	0.0145
	b	0.0147	0.0147	0.0148	
$u = 0.01, Pe = 100$	a	5.0705e−5	5.0436e−5	5.0474e−5	2.7001e−5
	b	3.6135e−6	3.8034e−6	5.7982e−5	
$u = 0.01, Pe = 1000$	a	9.9164e−5	9.8896e−5	9.9038e−5	3.9332e−4
	b	9.3053e−5	9.2760e−5	3.2735e−5	
$u = 0.1, Pe = 10$	a	0.0142	0.0142	0.0142	0.0144
	b	0.0146	0.0146	0.0146	
$u = 0.1, Pe = 100$	a	6.1848e−5	6.1545e−5	6.1698e−5	3.7516e−4
	b	2.0421e−6	2.0791e−6	6.4134e−5	
$u = 0.1, Pe = 1000$	a	1.0873e−4	1.0842e−4	1.0859e−5	4.7777e−4
	b	1.0206e−4	1.0182e−5	4.3888e−5	
$u = 1.0, Pe = 10$	a	0.0091	0.0091	0.0091	0.0108
	b	0.0101	0.0101	0.0102	
$u = 1.0, Pe = 100$	a	9.8746e−5	9.8425e−5	9.8595e−5	0.0032
	b	4.1051e−6	3.2676e−6	9.4699e−5	
$u = 1.0, Pe = 1000$	a	1.2979e−4	1.2956e−4	1.2966e−5	0.0031
	b	1.1923e−4	1.1968e−5	1.2775e−5	
$u = 1.0, Pe = 10\,000$	a	1.3726e−4	1.3716e−4	1.3721e−5	0.0031
	b	1.2820e−4	1.2892e−5	1.4238e−5	

In simulations, we still choose 256×256 grids and $\Delta t = 0.001$ in contrast with the simulation results of the first test problem, and set $u_1 = u_2 = u$. Table 2 shows the comparison of global relative error between our scheme and Model 1 with different parameters at 1000 time steps. From Table 2 we can see that when u is small Eq. (24) is approximate to Eq. (20) and the global relative errors of our scheme and Model 1 are little difference from those in Table 1. When u is large and the convection dominates the diffusion, the global relative errors of our scheme are much smaller then those of Model 1.

To test the accuracy of our scheme and Model 1 further, simulations are performed for $u_1 = u_2 = u = 1.0$ and different grid sizes: 32×32, 64×64, 128×128 and 256×256, corresponding to the time steps 0.01, 0.0025, 0.00625, 0.00015625, respectively. Fig. 1 gives the log–log plots of the global relative errors vs. space steps at $t = 1.0$ for different schemes and Pe numbers. The slopes of lines in the figure are all about -2.0. From the figure it is found that the errors of our scheme are clearly less than those of Model 1, and as Pe increases the errors of three schemes for computing $\overline{D}_i F_i$ tend to be the same.

4. Conclusion

In conclusion, we have proposed a new scheme for source term in LBGK model for convection–diffusion equation. Unlike the existing models (in the form of Model 1), our scheme only require the source term in order of the Knudsen number. This makes the scheme may have a wider range of application. Numerical tests are carried out for diffusion equation with source term and convection–diffusion equation with source term. It is found that the simulation results are in excellent agreement with the analytical solutions, which shows that the LBM has potentials to simulate CDE in some extent. It is also shown that the numerical accuracy of our scheme is generally much better than that of the model proposed previously. Because of the relationship between CDE with source term and RDE, the new scheme proposed in this paper can also be applied to RDS directly.

It should be noted that the new scheme proposed has several forms by selecting parameter θ in $\overline{D}_i F_i$ and using different computing schemes for $\overline{D}_i F_i$ in Eq. (2), which makes the new scheme flexible. Moreover, although the new scheme is only used for CDE with constant convection velocity and in LBGK model, it may be applied to other LB models for general CDE, such as Ginzburg's model [17].

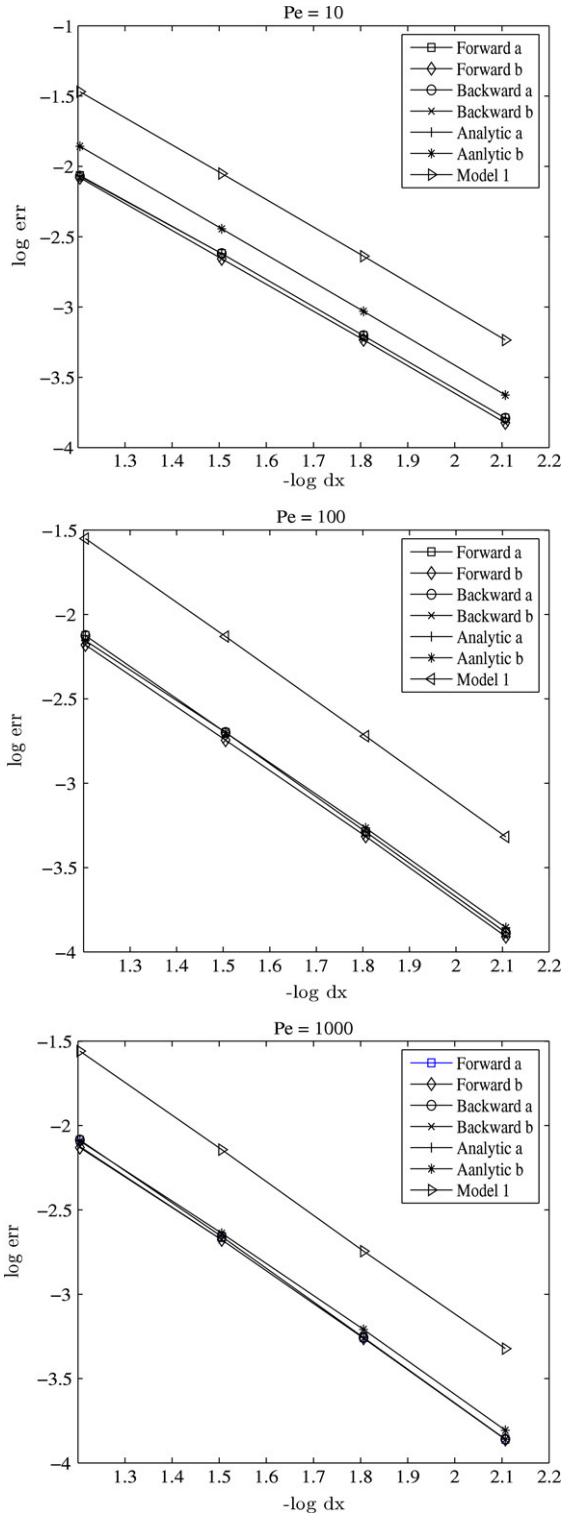

Fig. 1. Global relative errors vs. space steps at $t = 1.0$.

Acknowledgments

The authors thank the reviewers for their helpful comments and suggestions. This work was supported by the National Natural Science Foundation of China (Grant No: 70271609).

References

[1] Y. Qian, S. Succi, S. Orszag, Recent advances in lattice Boltzmann computing, Annu. Rev. Comput. Phys. 3 (1995) 195–242.
[2] Y. Qian, Simulating thermohydrodynamics with lattice BGK models, J. Sci. Comput. 8 (1993) 231–241.
[3] B.C. Shi, Z.L. Guo, N.C. Wang, Lattice Bhatnagar–Cross–Krook simulations of turbulent natural convection in a cavity, Chinese Phys. Lett. 19 (2002) 515–517.
[4] C.H. Sun, Lattice-Boltzmann models for high speed flows, Phys. Rev. E 58 (1998) 7283.
[5] Z.L. Guo, T.S. Zhao, Lattice Boltzmann model for incompressible flows through porous media, Phys. Rev. E 66 (2002) 036304.
[6] Y.S. Xu, Y.J. Zhong, G.X. Huang, Lattice Boltzmann method for diffusion–reaction–transport processes in heterogeneous porous media, Chinese Phys. Lett. 21 (2004) 1298–1301.
[7] H.P. Fang, S.Y. Chen, Lattice Boltzmann method for three-dimensional moving particles in a Newtonian fluid, Chinese Phys. 13 (2004) 47–53.
[8] A.J.C. Ladd, R. Verberg, Lattice-Boltzmann simulations of particle-fluid suspensions, J. Stat. Phys. 104 (2001) 1191–1251.
[9] S.P. Dawson, S.Y. Chen, G.D. Doolen, Lattice Boltzmann computations for reaction–diffusion equations, J. Chem. Phys. 98 (1993) 1514–1523.
[10] R. Blaak, P.M. Sloot, Lattice dependence of reaction–diffusion in lattice Boltzmann modeling, Comput. Phys. Comm. 129 (2000) 256–266.
[11] Z.L. Guo, B.C. Shi, N.C. Wang, Fully Lagrangian and lattice Boltzmann methods for the advection–diffusion equation, J. Sci. Comput. 14 (3) (1999) 291–300.
[12] X.Y. He, N. Li, B. Goldstein, Lattice Boltzmann simulation of diffusion–convection systems with surface chemical reaction, Mol. Simulat. 25 (3–4) (2000) 145–156.
[13] R.G.M. Van der Sman, M.H. Ernst, Advection–diffusion lattice Boltzmann scheme for irregular lattices, J. Comput. Phys. 160 (2) (2000) 766–782.
[14] G.W. Yan, A lattice Boltzmann equation for waves, J. Comput. Phys. 161 (9) (2000) 61–69.
[15] X.X. Zhang, A.G. Bengough, J.W. Crawford, I.M. Young, A lattice BGK model for advection and anisotropic dispersion equation, Adv. Water Res. 25 (2002) 1–8.
[16] I. Rasin, S. Succi, W. Miller, A multi-relaxation lattice kinetic method for passive scalar diffusion, J. Comput. Phys. 206 (2005) 453–462.
[17] I. Ginzburg, Equilibrium-type and link-type lattice Boltzmann models for generic advection and anisotropic-dispersion equation, Adv. Water Res. 28 (11) (2005) 1171–1195.
[18] D. d'Humires, Generalized lattice Boltzmann equations. AIAA rarefied gas dynamics: Theory and simulations, Prog. Astronaut. Aeronaut. 59 (1992) 450–548.
[19] P. Lallemand, L.S. Luo, Theory of the lattice Boltzmann method: Dispersion, dissipation, isotropy, Galilean invariance, and stability, Phys. Rev. E 61 (2000) 6546–6562.
[20] Z.L. Guo, C.G. Zheng, B.C. Shi, Discrete lattice effects on the forcing term in the lattice Boltzmann method, Phys. Rev. E 65 (2002) 046308.
[21] Z.L. Guo, C.G. Zheng, B.C. Shi, Non-equilibrium extrapolation method for velocity and pressure boundary conditions in the lattice Boltzmann method, Chinese Phys. 11 (2002) 366–374.